Mohaghegh et al., *BioImpacts.* 2025;15:30286
doi: 10.34172/bi.30286
https://bi.tbzmed.ac.ir/

Stimuli-responsive synthesis of silver nanoparticles applying green and chemical reduction approaches

Seraj Mohaghegh[1,2], Karim Osouli-Bostanabad[1,2], Hossein Nazemiyeh[1], Yadollah Omidi[3], Hossein Maleki-Ghaleh[1*], Mohammad Barzegar-Jalali[4*]

[1]Research Center for Pharmaceutical Nanotechnology, Faculty of Pharmacy, Tabriz University of Medical Sciences, Tabriz, Iran
[2]Students Research Committee, Tabriz University of Medical Sciences, Tabriz, Iran
[3]Department of Pharmaceutical Sciences, College of Pharmacy, Nova Southeastern University, 3200 S University Drive, Fort Lauderdale, FL, 33328, USA
[4]Pharmaceutical Analysis Research Center, Tabriz University of Medical Sciences, Tabriz, Iran

Article Info

Article Type:
Original Article

Article History:
Received: 8 Feb. 2024
Revised: 24 Jun. 2024
Accepted: 2 Jul. 2024
ePublished: 13 Aug. 2024

Keywords:
Stimuli-responsive
Environmental benign
Green chemistry
Silver nanoparticles

Abstract

Introduction: The current study reports the comparative stimuli-responsive synthesis of silver nanoparticles (AgNPs) with various sizes and morphologies employing *Lycium ruthenicum* extract and sodium citrate solutions.

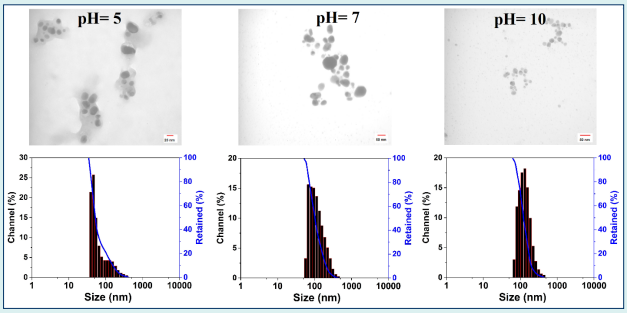

Methods: The morphology and size of AgNPs were regulated by varying the pH values, concentrations of the extract solution, and temperatures in the reaction medium. The prepared AgNPs were assessed via various instrumental analyses, including UV-Vis, FTIR, XRD, TEM, and DLS.

Results: The *L. ruthenicum* extract displayed several functional groups that reduced the Ag ions to the AgNPs at different values of pH. However, the primary chemical structure of *L. ruthenicum* was virtually unaltered at these conditions. Variations in the pH and extract concentration of the reaction medium yielded AgNPs of different sizes and morphologies. Both bio- and chemo-synthesized AgNPs revealed a relatively dispersed sphere-shaped morphology under alkaline conditions (≈ 36 nm).

Conclusion: This study introduced a simple, valuable, and green technique for stimuli-sensitive AgNPs synthesis employing the *L. ruthenicum* extract.

Introduction

Silver nanoparticles (AgNPs), offering unique characteristics, have been investigated to serve many applications, including the development of nanoscale therapeutics for cancer therapy.[1] Once used, AgNPs can be found in the body as Ag^+ ions inducing the reactive oxygen species (ROS) production, leading to damaging tumor cells.[2] In this context, the characteristics of as-synthesized AgNPs are mainly determined by various techniques. Accordingly, the size, structure, and consequent physical, chemical, as well as biological features greatly depend on the synthesis process; hence, there is an enormous variety of synthesis methods.[3-5] Typically, AgNPs synthesis can be categorized into physical, chemical, and biological approaches. The physical techniques do not use toxic chemicals, are usually fast, and produce AgNPs with a narrow size distribution. Despite this, the problem with such procedures is the considerable amount of energy consumed in the process.[6] The chemical techniques can be divided into electrochemical, irradiation-assisted, pyrolysis, and chemical reduction methods.[7-9] The Ag^+ ions' reduction to Ag^0 with the help of such reducing agents as $NaBH_4$, ascorbate, and citrate (standard procedure advanced by Turckevich), referred to as chemical reduction, which is the most applied and broadly reported approach for AgNPs synthesis.[10] In the process developed by Turckevich, the citrate serves as a reducing and stabilizing (electrostatic stabilization)

*Corresponding authors: Mohammad Barzegar-Jalali, Email: mahbarja@gmail.com; Hossein Maleki-Ghaleh, Email: hossein.maleki85@gmail.com

agent of Ag^+ions to corresponding Ag particles. This phenomenon could double the electric layer established on AgNPs surface, preventing their agglomeration.[11] However, the recognized procedures for synthesizing AgNPs employ environmentally-hazardous and toxic reagents. Consequently, researchers have proposed some alternatives to such chemical methods; this mostly consists of replacing the more established reducing compounds with those which are natural. Such approaches can be regarded as "green bio-assisted synthesis" since they abide by the green chemistry principles. Many researchers are currently using this approach as some novel method for AgNPs synthesis, which is defined as the "development of economic chemical processes and products for the purpose of decreasing or completely abandoning the use and production of dangerous materials".[3,4,7,12-14] AgNPs synthesis employing the green chemistry can be accomplished using (i) templates (e.g., viruses, membranes, and DNA); (ii) microorganisms (e.g., fungi, bacteria, and actinomycetes), and (iii) plants and their extracts.[15]

As a non-pathogenic technique used for the synthesis of AgNPs, the use of plants as well as their extracts is a direct, one-step process offering a greater capacity for bio-reduction, in comparison to using microorganisms and templates.[16] Various plants have successfully been employed to synthesize stable bioactive and biocompatible AgNPs with potential therapeutic applications.[17-19] The whole plants or their extracts can be used to produce AgNPs; however, the reducing component availability is highly focused on in the extract solution compared to the entire plant. Therefore, most investigations have concentrated on the use of plant extracts. Available biomolecules in these extracts (i.e. terpenoids, ketones, phenolic compounds, alkaloids, aldehydes, carboxylic acids, and amines) could be utilized as reducing agents of metallic ions to the corresponding nanoparticles (NPs) in a straight green synthesizing method. Flavones, quinones and organic acids have involvement in the immediate reduction of Ag^+ions to Ag° in the reaction medium.[20] The creation of base metal from its metallic ions benefiting these water-soluble biological reducing factors is comparatively fast, easily directed at ambient pressure, and can be scaled up. These compounds might act as reducing and stabilizing agents in the formation of NPs, where it is believed that the plant extract origin affects the synthesized NPs' characteristics because different extracts have varied concentration and mixture of reducing factors.[21-23]

Many studies have investigated berry fruits, and the *Lycium* plant dried fruits (*Fructus lycii*, *Wolfberries*, *Goji berries*) in Asian and other countries.[24] There are about 80 kinds of Solanaceae (*Lycium L*) generally,[25,26] nonetheless, only three kinds (*L. barbarum*, *L. chinense*, and *L. ruthenicum*) are used as a remedy. Research have shown that *L. ruthenicum* has several medical effects, such as antioxidant,[27] immune-enhancing,[28] anti-fatigue,[29] and anti-aging.[29] Studies have shown that *L. ruthenicum* consists of different bioactive compounds, like polysaccharides, alkaloids, phenolic acids, anthocyanin, flavonoids, carotenoids, fatty acids and essential oils.[30]

Currently, no scientific report is available on the synthesis of AgNPs using the extract of *L. ruthenicum* as a capping and reducing agent. Since phenolic compounds, such as phenolic acids and flavonoids, are abundant in *L. ruthenicum* extract, the aim of present study is on the applicability of this herbal compound in the synthesis of AgNPs with controlled morphology and size. The main goals of the current work were:

- The synthesis of AgNPs through a green nanotechnology procedure benefiting the extract of *L. ruthenicum*.
- The synthesis of AgNPs benefiting citrate as a reducing agent in the chemical procedure.
- The optimization of pH value, concentration, and temperature of reducing agent to synthesize AgNPs with controlled physicochemical features.
- The assessment of these physicochemical characteristics.

In short, this study is invaluable since it compares two distinct methods for the synthesis of AgNPs and introduces a novel reducing agent to stabilize and synthesize AgNPs.

Materials and Methods

In this work, the whole solvents as well as chemical substances were provided by Sigma-Aldrich (St. Louis, Missouri, USA) and used without any further purification due to their laboratory-grade purity. Besides, ultra-pure Milli-Q water with the particular resistivity of 18.2 MΩ.cm was used as a solvent in all tests.

Preparation of L. ruthenicum extract

The plant of *L. ruthenicum* was obtained from the University of Tabriz campus, Tabriz, Iran. The identification of *L. ruthenicum* was directed at the herbarium of Tabriz University of Medical Sciences, TbzMed herbarium sample number: 4039 (tbz-fph). After identification, 1000 g of *L. ruthenicum* fruit was washed by distilled water for the removal of any possible impurities and dust. About 600 g of *L. ruthenicum* fruit was pressed and plunged in 70% ethanol with a 1:3 w/v ratio of *L. ruthenicum*: ethanol at room temperature for a period of 72 h, while shaking (300 RPM) was done. The filtration of extract was done using the #1 Whatman paper filter (Sigma-Aldrich, Missouri, USA). Afterward, a rotary evaporator (Heidolph Persia, Tehran, Iran) with low pressure was employed to condense the filtered extract using reduced pressure to eliminate ethanol at 40 °C. Ultimately, the dried and condensed extract was weighed precisely and kept at 4 °C.

Green synthesis procedure

Regarding the synthesis procedures using chemical and biological reducing agents, to examine and optimize the efficiency of these procedures in various pH values (including 5, 7 and 10), several tests were then conducted at 85 °C. Briefly, before adding *L. ruthenicum* extract (5% w/v), 10 mL of $AgNO_3$ solution (1 mM) (pH = 5) was heated to reach the preferred temperature. Moreover, 0.1 -N sodium hydroxide was used to maintain the $AgNO_3$ solution's pH at the desired value. Following the adjustment of pH, addition of 1 mL of the *L. ruthenicum* extract solution to $AgNO_3$ solution was done in a drop-wise manner; the resulting mixture was left for about 20 min, constantly agitated to fulfill the Ag^+ ions reduction to Ag°. The solution's color changed from yellowish to red, thus indicating the Ag° particles formation. Finally, centrifuging of the obtained suspension was done three times for 15 minutes at 13000 RPM; it was employed for additional applications and analyses.

Chemical synthesis procedure

In relation to the chemical process of synthesizing AgNPs, sodium citrate, as one of the most common reducing compounds, was used in the wet chemical technique to be compared with the biosynthesizing method. A 1% w/v solution of sodium citrate was prepared by dissolving 1 g of trisodium citrate in 100 mL of distilled water and hired as the reducing factor. The stages of synthesizing Ag particles via chemical route are identical to the green one.

Characterization

UV-vis study

The UV-visible spectrometry of synthesized colloidal solutions was conducted, using the Shimadzu spectrophotometer (Kyoto, Japan) with a 60 nm/min scan rate in the 400-700 nm range to identify the existence of excitation spectra (surface plasmon resonance). The solutions mentioned above were poured in 1-cm length path quartz cuvettes to conduct the test.

Fourier-transform infrared analysis (FT-IR)

Greenly-synthesized nanoparticles were examined with a Shimadzu FT-IR spectrophotometer (Shimadzu 43000, Kyoto, Japan), and their FT-IR spectra were recorded. Regarding the test, the particles were compressed in a disk shape, employing the method of KBr disk and examined with average spectra of 32 scans at the 2 cm^{-1} resolution in the 4000-600 cm^{-1} scanning range.

X-ray diffraction (XRD) examination and energy-dispersive x-ray (EDX) spectroscopy

The patterns of XRD belonging to the synthesized particles' were assessed using x-ray diffractometer D 5000 (Siemens, Munich, Germany) in a 2θ angle of the 10-85 ° range; it was done at a step size and scanning rate of 0.02° and 0.6°/min, respectively. The Cu Ka radiations (λ = 1.5405 Å) at 40 kV and 30 mA were then used as operational parameters. The elemental composition of *L. ruthenicum*-AgNPs was ascertained by EDX which was matched with the FE-SEM (MIRA3, Tescan Co., Brno, Czech).

Transmission electron microscopy (TEM) and dynamic light scattering assessments (DLS)

The morphology as well as size of synthesized particles were measured by using TEM (20 G2 Tecnai 80 kV, Zaragoza, Spain). The process of sample preparation for the purpose of TEM analysis included placing a drop of *L. ruthenicum*-AgNPs solution on a copper grid with carbon coat (300 meshes) and allowing it to dry for a period of 30 min at ambient temperature. An instrument for DLS test (Nanotrac Wave, Microtrac, Colorado, USA) was then used for the estimation of polydispersity index (PDI) and average particle size of synthesized AgNPs.

Results and Discussion

UV–vis absorption analysis

Chemically and eco-friendly synthesis of the AgNPs was carried out using *L. ruthenicum* extract and citrate solutions in the current study. The AgNPs formation through the Ag^+ ions reduction to Ag° was visually confirmed by the alteration in the color of $AgNO_3$ solution after adding the reducing solutions from yellowish to colloidal brown. Earlier studies have suggested the AgNPs formation with the use of plant extracts as well as citrate solutions. The reduction of the Ag^+ ions to AgNPs by suitable reduction agents could lead to the formation of characteristic surface plasmon resonance (SPR) band, revealing the reduction capability of these compounds. Research on different metal NPs have suggested that the shape and position of the SPR peaks firmly depend on their morphology, size, and agglomeration state.[3,11,16,17,31,32] In the current study, while definitive absorption peaks which were in the 400–450 nm range indicated the existence of bio- and chemo-synthesized AgNPs SPR, there were not any remarkable absorption peaks of *L. ruthenicum* extract and citrate solutions in the visible region. Fig. 1 illustrates the spectral UV-vis absorption results of the synthesized AgNPs benefiting *L. ruthenicum* aqueous extract as well as sodium citrate 1% w/v solution in 1 mM solution of $AgNO_3$ at various pHs and controlled temperatures for 20 min of incubation.

In this work, different factors, including *L. ruthenicum* extract's concentrations (2.5-7.5% w/v), pH values (5-10), and temperature of reduction solutions (45-85 °C) were optimized, as factors influencing the size, morphology, and yield of AgNPs. Fig. 1 (a, b, and c) depicts the observed UV-vis spectra of $AgNO_3$-*L. ruthenicum* extract reaction's colloidal suspension according to the reaction temperatures (including 45, 65 and 85 °C, respectively). Regarding Fig. 1a, the SPR band of synthesized AgNPs is positioned at about 422 nm, 438 nm, and 447 nm at pH values of 10, 7, and 5, respectively. The SPR bands' intensity

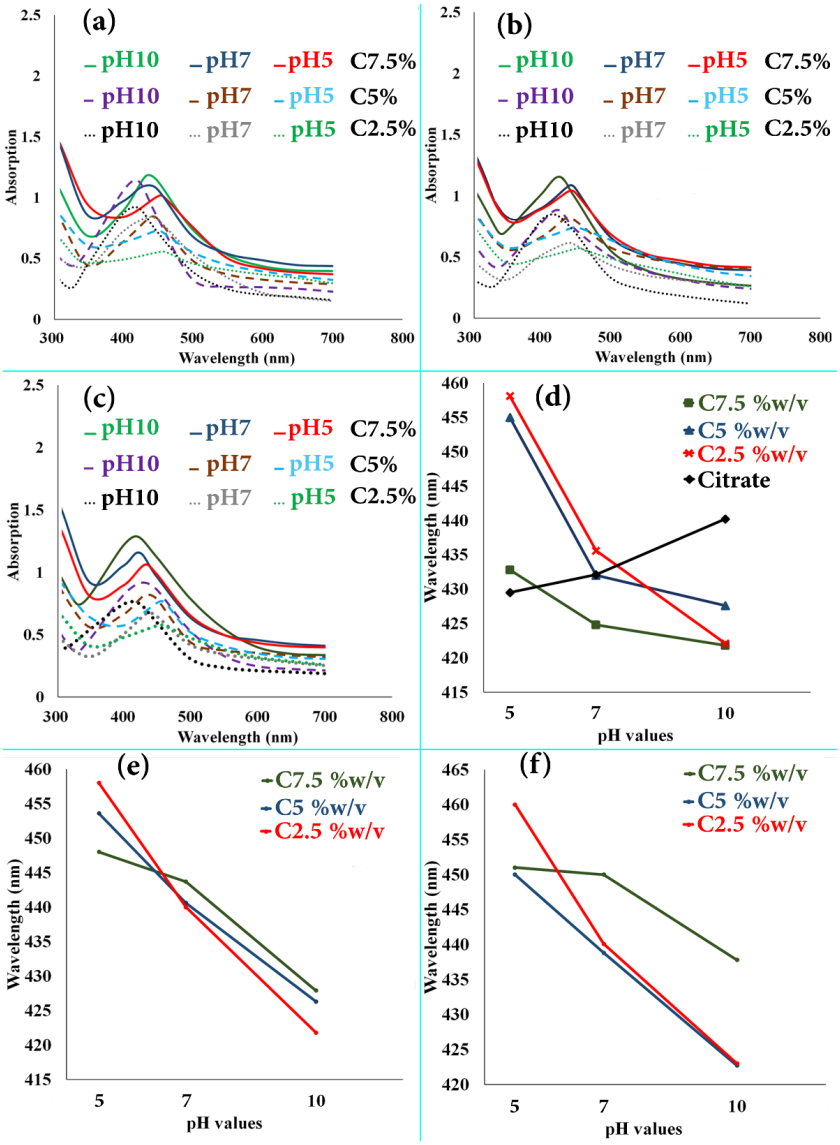

Fig. 1. The UV–visible absorption spectra for AgNPs synthesized at different treatment temperatures, extract concentrations, and pH values for 20 min by the sodium citrate (1% w/v) and *L. ruthenicum* extract solutions; (a) T = 45 °C, (b) T = 65 °C, and (c) T = 85 °C. The graphs of surface plasmon resonance band wavelength changes affected by pH values'; (d) T = 85 °C, (e) T = 65 °C, and (f) T = 45 °C.

enhanced as the *L. ruthenicum* extract concentration increased in the reaction medium. Fig. 1b illustrates the same trend in which the SPR band of AgNPs, as a function of *L. ruthenicum* extract's concentration, increased in intensity with an increase in the extract concentration in the colloidal suspension.

Fig. 1c corresponds to the SPR plots of colloidal suspensions at 85 °C, indicating the same trend as the two previous groups. Regarding these data (Fig. 1a-c), it is implied that the enhancement in the concentration up to 7.5% w/v led to the increased rates of deposited Ag yield. Moreover, regarding the minor shifts in the characteristic SPR peaks, it is apparent that the rise in concentration of extract did not significantly affect the colloidal AgNPs' principal size. The abovementioned results could be corroborated by the fact that the Ag^+ions' reduction via *L. ruthenicum* carboxylate (COO–) groups at higher pH value was more effective than the lower one, leading to the enhancement of AgNPs size in the aqueous solution (Fig. 2). As illustrated in Fig. 1 (panels a-c), an increase in the solution's pH increased the absorbance of colloidal suspension, demonstrating the higher yield of AgNPs. The spectral assessment of the samples decreased with the use of *L. ruthenicum* extract solutions, indicating that the UV SPR peaked at a range of 420-450 nm. This range is generally associated with the SPR peaks of AgNPs, in which their intensity increased as the value of pH enhanced from 5 to 10 with a blue-shift in the peaks' position (Fig. 1 d, e, and f, corresponding to the T = 85 °C, 65 °C, and 45 °C, respectively). The quantum confinement influence is the reason behind the SPR band blue-shift and enhancement of the oscillator strength, indicating an increased size of particles.[30] This can be attributed to the inadequacy of extract molecules in capping the Ag

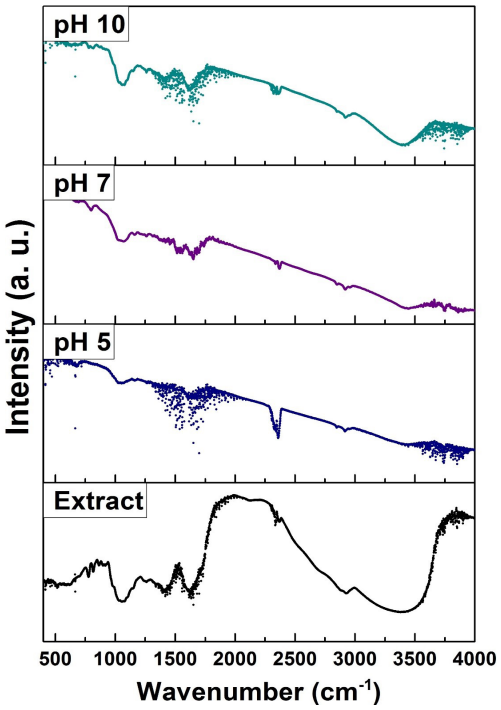

Fig. 2. *L. ruthenicum* extract FT-IR spectra before and after synthesizing under different pH amounts at 85 °C.

nanoclusters further developed, thus demonstrating that optimizing the quantity of both extracts and $AgNO_3$ solutions that are added to a specific pH is important. In the present research, some biomolecules in *L. ruthenicum* extract are responsible for reducing Ag^+ to Ag^0, which are yet-to-be recognized (Fig. 2). The as-synthesized AgNPs growth using a chemo-synthesizing agent (1% sodium citrate) was also investigated.

As represented in Fig. 1d, the UV-Vis spectra of the abovementioned samples indicate an apparent increase in the SPR absorbance wavelength and a redshift in the peaks' position by an increase in pH values from 5 to 10. AgNPs with the morphology of semi-spherical and a diameter of around 50 nm, represent a distinctive SPR absorption peak at 429 nm. The diameter enlargement and rise in the polydispersity index of synthesized NPs lead to the redshift of this band to the wavelengths which are longer. However, the decrease in the synthesized NPs diameter results in a blue-shift and positioning of the peak at lower wavelengths (Fig. 1d-f). The results above are consistent with previous research.[3,11,17,33] The formation procedure and particle size of chemo-synthesized and bio-synthesized AgNPs highly depend on the pH of synthesizing solutions. Accordingly, the optimum pH value to achieve highly uniform AgNPs in terms of particle size and spherical morphology was 10. It was further corroborated by the results obtained from microscopic and DLS assessments.

FTIR data analysis

FTIR analysis can be conducted to identify the existence of some functional groups in *L. ruthenicum* extract. Furthermore, it can confirm the extract solution's dual function as a reducing and capping compound of AgNPs. Therefore, the FTIR analysis was performed to detect the possible bounded functional groups on the synthesized AgNPs. Fig. 2 illustrates the FTIR spectrum of AgNPs synthesized using the extract solution of *L. ruthenicum* (7.5% w/v) at pH values of 5, 7, and 10 at 85 °C for 20 minutes and the spectrum of *L. ruthenicum* extract alone.

Numerous functional groups of *L. ruthenicum* extract were identified, but IR bands at around 1061, 1412, 1629, 2357, 2928, and 3409 cm^{-1} were more prominent among the others. It is believed that these noticeable bands originated from the different biomolecules existing in the *L. ruthenicum* aqueous extract. These spectral bands can be ascribed to the C-O-H stretching vibrations, symmetrical COO− (amide C=O), asymmetrical COO−, alkanes group's -CH, and the -OH stretching vibrations of functional groups in phenolic compounds, respectively.[3,7,32]

The broad IR band between 3550 and 3000 cm^{-1} can be associated with the N-H stretching vibration of group OH, and NH_2 stretching vibration overlapping is attributed to *L. ruthenicum* extract and water molecules.

Regarding the treated samples' FTIR spectra, it has been demonstrated that the Greenly-synthesized ones have the polyphenolic –OH, alkane groups -CH stretching vibrations, and the carboxylic acid group stretching. These data proposed that the previously mentioned functional groups of biomolecules in *L. ruthenicum* extracts were active in reducing Ag ions to the consequent AgNPs. Similarly, regarding the results of AgNPs biosynthesis using the extract of *Sargassum polycystum*, it is believed that the aforementioned functional groups were involved in the biosynthesis procedure.[34] These outcomes imply that the bioactive groups in *L. ruthenicum* extract could be chiefly involved in Ag ions stabilization into AgNPs. The slight shifts in the FTIR spectra could be ascribed to the interaction of Ag ions with *L. ruthenicum* extract's functional groups. Moreover, the appearance of FTIR peaks in the samples synthesized at 85 °C at diverse pHs (including 5, 7 and 10) in the proximity of *L. ruthenicum* characteristic peaks demonstrated that no changes in the original FTIR spectrum of *L. ruthenicum* occurred after treatment, suggesting that *L. ruthenicum*'s main chemical structure was mainly reserved.

The essential biomolecules in *L. ruthenicum* are polysaccharides, alkaloids, phenolic acids, anthocyanin, flavonoids, carotenoids, fatty acids and essential oils. The hydroxyl groups, alkaloids, and flavonoids are responsible for the biosynthesis of AgNPs. In this regard, the formation of hydrated electrons by hydroxyl groups present in the extract of *L. ruthenicum* resulted in the Ag^+ ions reduction to Ag^0.[35] Moreover, the Ag^+ ions are grasped on the surface of alkaloids. They are reduced by

other bioactive compounds, leading to the materialization of Ag nuclei. Then, these Ag nuclei accumulated, grew in size and created AgNPs.[32,36] As secondary metabolites within the flavonoids of *L. ruthenicum* extract, the polyhydroxy groups are the other major reducing mediators contributing to the reduction of Ag ions to corresponding AgNPs.[37] The groups mentioned above have a vital role in the antioxidant properties of flavonoids with metal ion chelating and free radical scavenging characteristics.[31,37] To put it differently, the reduction and antioxidant characteristics of flavonoids are attributed to their atoms of hydrogen and the capacity to donate electrons. Therefore, the formation of AgNPs using *L. ruthenicum* biomolecules might result from the chelation of Ag^+ions, which is also associated with the easy transmission of electrons from an oxidant to a reductant state.[33]

The overarching mechanism in which the Ag^+ions were reduced to Ag° in the chemo-synthesis approach at an elevated temperature could be explained using the following equation:

$$C_6H_5O_7^{3-} + 2Ag^+ \rightarrow C_5H_4O_5^{2-} + H^+ + CO_2 + 2Ag^0$$
$$(C_5H_4O_5^{2-} = {}^-OOCCH_2COCH_2COO^-)$$

Citrate has various functions in the process of AgNPs synthesis. Through tight coordination with Ag^+ions, citrate can form some Ag^+-citrate complex (pK1 = 7.1) at ambient temperature. However, it produces Ag metal particles as reducing agents at high temperatures. Moreover, citrate preserves the produced nuclei of Ag by acting as a capping agent. The chemically-synthesized AgNPs' homogeneous nucleation mechanism and their kinetic aspects are reported in the studies. The formation of colloidal particles under homogeneous nucleation in the solution happens through several steps. It can be explained as follows: (I) the process of nucleation, particularly the creation of Ag° atoms with the nuclei formation ($nAg^+ \rightarrow nAg^0 \rightarrow Ag_n^0$), and regarding the step-by-step mechanism (i.e. $Ag^+ \rightarrow Ag^0 \rightarrow Ag_2^+ \rightarrow Ag_4^{2+} \rightarrow \ldots \rightarrow Ag_n^0$), the nucleation process rate is controlled by the Ag ions' chemical reduction rate. (II) Following a new phase of nucleus creation, the growth of NPs begins, which can take place both as a coagulative mechanism (i.e. $mAg_n^0 \rightarrow Ag_{n.m}^0$) and reduction of Ag ions on the nucleus surface ($Ag_n^0 + Ag^+ + e^- \rightarrow Ag_{n+1}^0$). Undoubtedly, in practical systems, all these reactions will coincide one after another and accomplish each other. The mechanisms and kinetics of AgNPs formation from a silver nitrate solution by applying the solution of sodium citrate as a reducing agent are available in more detail in the literature.[11,38,39]

XRD and EDX studies

The XRD test was performed to examine the phase configuration and crystalline shape of AgNPs synthesized through bio- and chemo-synthesized methods. Fig. 3a depicts the XRD patterns belonging to AgNPs synthesized using the *L. ruthenicum* extract solutions at pH = 5-10 and 1% citrate. Regarding the databank of the Joint Committee on Powder Diffraction Standard (JCPDS No. 04-0783 and No. 03-0921), all significant peaks depicted in Fig. 3a could be considered as silver crystals' face-centered cubic (FCC) shape, with the lattice constant being a = 4.08 Å. The distinctive and sharp peaks in the XRD patterns revealed the proper crystallization of the synthesized AgNPs. Furthermore, the four characteristic peaks at 77.50°, 64.80°, 46.60°, and 38.30° (2θ angles) can be associated with diffractions from the planes of (311), (220), (200), and (111), respectively. This is the result of Bragg's reflections from the silver's FCC crystal structure.

Evidently, the matching peak to the (111) plane is sharper than other Bragg reflections from the planes (200), (220), and (311), suggesting that the AgNPs are rather oriented along that specific plane. Additionally, the presence of some minor peaks at 2θ angles of 44.16°, 57.46°, and 67.36°, associated respectively with the diffractions from planes of (100), (103), and (006), was believed to reveal the hexagonal structures of Ag crystals. The biphasic nature of the synthesized AgNPs can be inferred from the observation mentioned above. There were also three unassigned peaks in the XRD pattern of the synthesized AgNPs at 28.2°, 32.6°, and 57.8° 2θ angles, which might be associated with the functional biological groups of *L. ruthenicum* extract. Accordingly, it implies that the crystallization of the bioorganic phase took place on the AgNPs surface.[17,31,40] It is possible to observe sharp diffraction peaks in a sample in which the diffraction patterns of powders usually demonstrate broad peaks assessed in degrees hundredths. The broadening of peaks results from the alterations in diffraction domain/crystallite size, the crystal lattice distortion, and the structural defections (i.e., stacking and twin faults). By considering Fig. 3a, it is evident that the peaks of XRD became borderline by elevating pH, proposing the AgNPs creation with reduced sizes.

The mean crystallite size of AgNPs formed in the bio-synthesized process was calculated using the Debye-Scherrer formula ($D = k\lambda / \beta \cos\theta$), where D, k, λ, β, and θ stand for the crystalline size average (Å), a constant value equal to 1, the x-ray source wavelength (1.54056 Å) used in XRD, the full width at half maximum (FWHM) intensity of the diffraction peak (radians), and Braggs angle, respectively. The mean size of the Ag nanocrystals was determined at a range of 15-35 nm at various pH values.

Fig. 3b depicts the characteristic EDX spectrum of bio-synthesized AgNPs using *L. ruthenicum* extract solution at pH = 5, accompanied by the percentage weight of its elements. The distinct silver absorption signal corresponding to the SPR of AgNPs was detected as a characteristic peak at around 3.0 keV. Moreover,

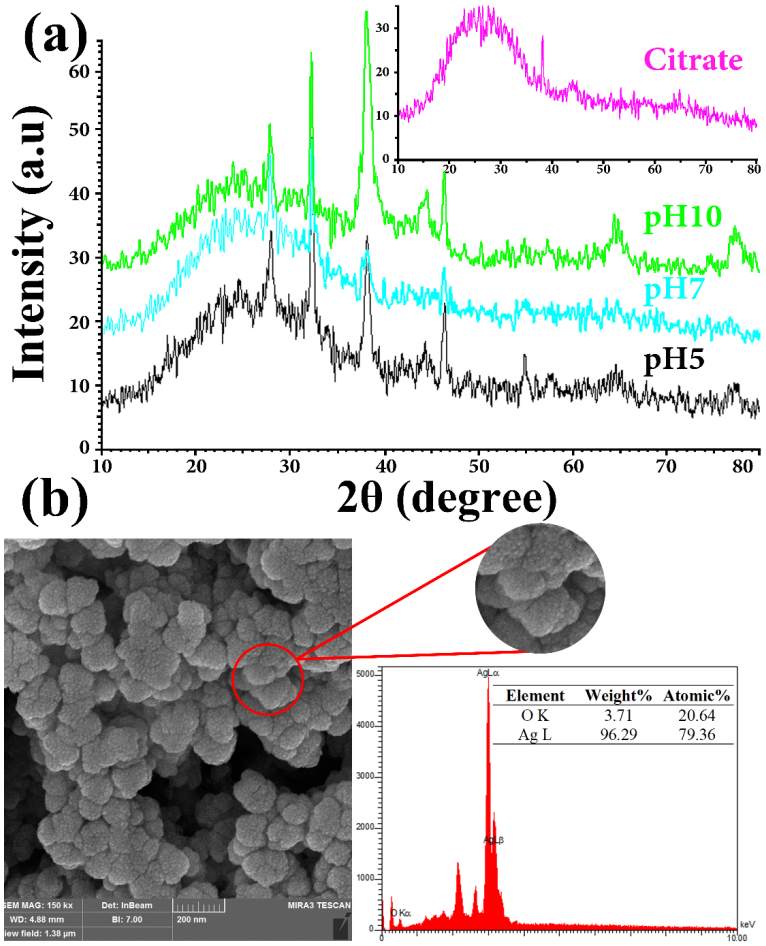

Fig. 3. (a) The synthesized AgNPs XRD patterns benefiting citrate and *L. ruthenicum* extract solutions in different pH at 85 °C; (b) As-synthesized AgNPs typical EDX pattern (by *L. ruthenicum* extract solution) at pH = 5.

some peaks related to O were also noted, probably triggered by the contribution of *L. ruthenicum* extract in the creation of AgNPs. Additionally, evaluation of the EDX spectrum revealed the metallic state of synthesized AgNPs without having the formation of Ag_2O in them and further impurities. The data attained from XRD and EDX are consistent with the results of UV-vis (Fig. 1), the morphological and particle size distribution assessments (Figs. 4 and 5), and previously published research demonstrating relatively the same results.[3,17,31,37,40]

Morphological and particles size distribution assessments

In order to study the microstructure and particle size distribution of AgNPs, TEM and DLS tests were performed. The morphologies, particle sizes, and synthesized samples PDI were evaluated. As shown, the influence of varying pH values and concentration of *L. ruthenicum* extract solution on the spectra of UV-vis (Fig. 1) and XRD data could be observed (Fig. 3), and the different particle sizes of synthesized AgNPs were corroborated by TEM and DLS observations (Figs. 4 and 5). Fig. 4 indicates the achieved data of AgNPs assessments prepared by applying the extract's diverse concentration: (a) 2.5% w/v, (b) 5% w/v, (c) 7.5% w/v, and (d) 1% citrate at 85 °C at pH = 5. As-synthesized AgNPs anisotropy led to the long-wavelength tail of the SPR plots, which is obvious from the TEM micrographs of the prepared AgNPs (Figs. 4 and 5).

Fig. 4 (a-d) shows the influence of various concentrations of the extract and reducing agents on particle size as well as the morphology of AgNPs. These images of AgNPs illustrate an increase in particle size with an increase in the *L. ruthenicum* extract concentration. Additionally, changing the reducing agent affected the synthesized AgNPs size (Fig. 4d), suggesting that *L. ruthenicum* and citrate must behave as a stabilizer and nucleation activator. Figs. 4c and 4d consist of almost large-diameter (about 50 nm) anisotropic particles with semi-spherical (polygonal) morphologies, whereas smaller nanoparticles were obtained at a lower *L. ruthenicum* extract concentration (Figs. 4a and 4b) with the mean diameter being approximately 16 nm. TEM images of bio-synthesized AgNPs using the extract of *L. ruthenicum* (7.5% w/v) at the temperature of 85 °C with different pH values (a) 5, (b) 7, and (c) 10 are depicted in Fig. 5.

Collectively, the outcomes of the current study showed the remarkable morphology and particle size dependence of AgNPs on the pH values and *L. ruthenicum* extract

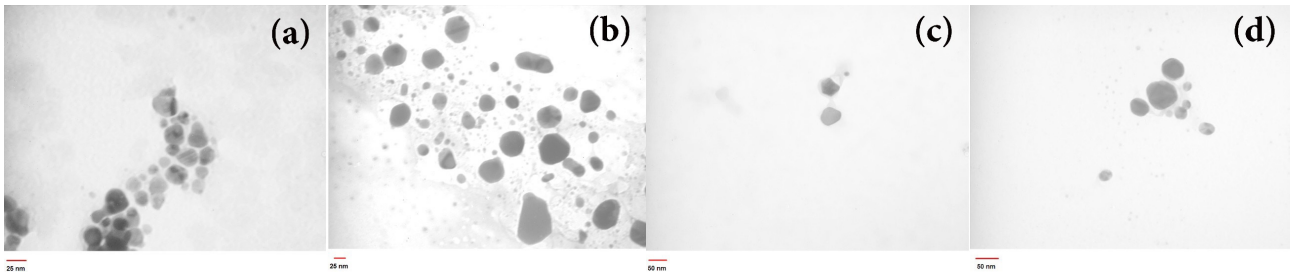

Fig. 4. The as-synthesized AgNPs TEM images employing *L. ruthenicum* extract at 85 °C under controlled pH = 5 with different extract concentrations (a) C = 2.5% w/v, (b) C = 5% w/v, (c) C = 7.5% w/v, and (d) 1% citrate solution

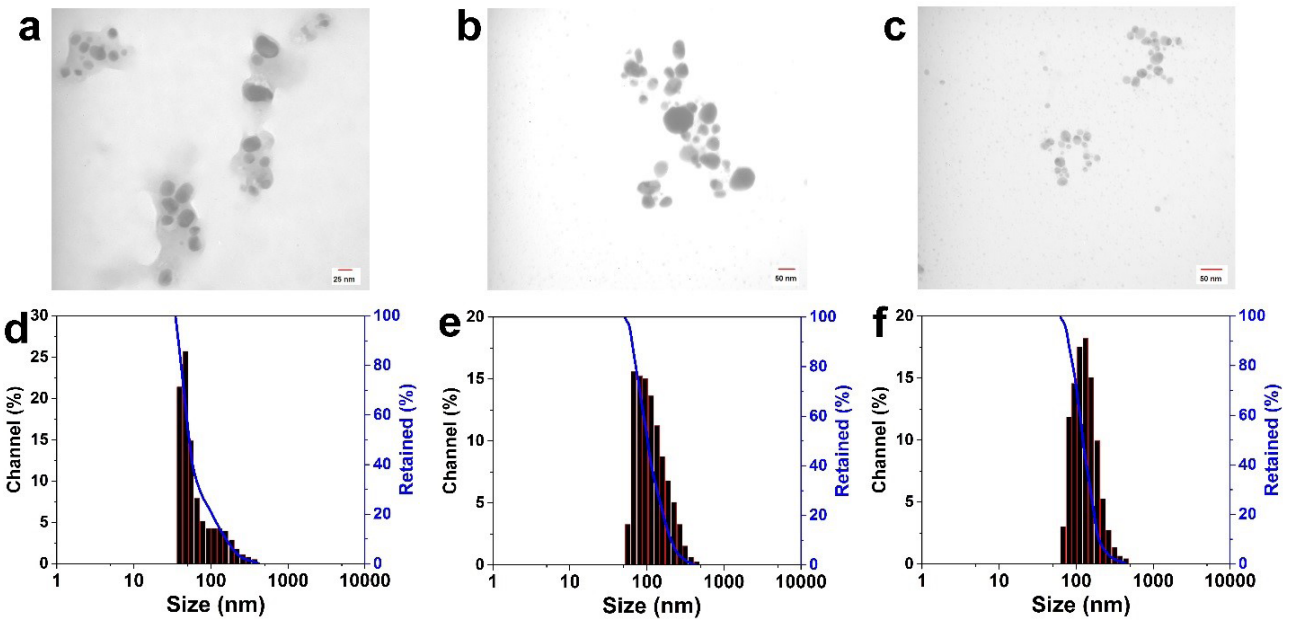

Fig. 5. The as-synthesized AgNPs TEM images employing *L. ruthenicum* extract at 85 °C under controlled pH values (a) pH = 5, (b) pH = 7, and (c) pH = 10; (d), (e), and (f) indicate histograms of size distribution (DLS data) related to images (a), (b), and (c), respectively

solutions. The TEM micrographs demonstrated that the biosynthesized AgNPs at a pH of 5 had a mean particle size of around 16 nm, mostly in a polygonal shape (Fig. 5a). The specimens prepared at pH = 7 displayed a semi-spherical morphology with the average particle size of about 25 nm (Fig. 5b), and the ones which were synthesized at pH = 10 displayed sphere-shaped morphology, with an average diameter being almost 36 nm (Fig. 5c). Considering the DLS results, the mean particle sizes of the prepared NPs were 125.2, 103.6, and 52.6 nm, corresponding to pH values of 10 (Fig. 5f), 7 (Fig. 5e), and 10 (Fig. 5f), respectively. The varied particle sizes demonstrated by the DLS and TEM analysis are associated with the particles' hydrodynamic diameter, which is calculated by the DLS test.

Regarding the *L. ruthenicum* extract's pH value, its increase from 5 to 10 led to an almost sphere-shaped morphology of the synthesized AgNPs and an increase in the size of the particles. The biosynthesized AgNPs PDI was revealed to be 3.91 at pH = 5, 2.481 at pH = 7, and 5.14 at pH = 10. These results propose that the effect of pH values on the morphology as well as size of the synthesized AgNPs might conform to the chain conformation alterations of *L. ruthenicum* under various pH conditions (Fig. 2). As mentioned before, the increase in the particles' diameter leads to a redshift in the SPR peaks. There was a slight shift in the spectral position of bio-synthesized samples' SPR peaks (Fig. 1), indicating the particle size distribution as revealed by TEM and DLS results (Figs. 4 and 5). It was also confirmed by other studies in which the shape and size of the synthesized AgNPs were affected by the adjustment of the pH values of reducing solutions.[40,41] Moreover, there was no alteration in the color and visual aggregation of synthesized solutions even after one month (data not presented here). Therefore, the biosynthesized AgNPs were evenly distributed and highly stable at different pH values (5–10). It was concluded from the present study that AgNPs with relatively uniform size distribution, spherical morphology, and larger mean particle size were synthesized at a pH of 10.

Conclusion

Comparative eco-friendly and chemically synthetic procedures for producing AgNPs using simple and

inexpensive compounds were reported. Various conditions under which the experimental methods were conducted in order to control the morphology, as well as size of the synthesized AgNPs, were outlined. A quick and green synthetic approach using *L. ruthenicum* extract has revealed great potential in AgNPs synthesis. Furthermore, probable mechanisms and functional groups responsible for the formation of AgNPs using 1% citrate and *L. ruthenicum* extract solutions were explained. The IR spectral profile of *L. ruthenicum* extract exhibited several functional groups originating from numerous biomolecules existing in the extract of *L. ruthenicum* that were more prominent among the others and reduced Ag ions to the consequent AgNPs. The pH values of the reducing solutions and *L. ruthenicum* extract concentrations were shown to have a vital role in the morphology as well as the size-controlled synthesis of AgNPs in aqueous solutions. More interestingly, the synthesized AgNPs using either bio- or chemo-synthesis methods had a fairly well-dispersed sphere-shaped morphology and larger particle size when synthesized under alkaline pH.[10] The abovementioned findings were based on the observations from UV-vis spectroscopy, DLS data, XRD graphs, and TEM images. These results revealed that the nontoxic and bio-derived *L. ruthenicum* extract could be utilized as a stabilizing and reducing agent for the stimuli-responsive AgNPs synthesis via green chemistry method applicable in a broad range of biomedicine and biotechnology-relevant industries. As presented in this study, the possibility of controlling the morphology as well as size of the AgNPs through the synthesis process opens up an opportunity to think of other biological agents capable of being used in the synthesis of metal nanoparticles.

Acknowledgements
This study was supported by the Elite Researcher Grant under award number #971166 from the National Institutes for Medical Research Development (NIMAD), Tehran, Iran.

Authors' Contribution
Conceptualization: Hossein Nazemiyeh, Yadollah Omidi.
Data curation: Seraj Mohaghegh.
Formal analysis: Seraj Mohaghegh, Karim Osouli-Bostanabad.
Funding acquisition: Mohammad Barzegar-Jalali.
Investigation: Karim Osouli-Bostanabad.
Methodology: Karim Osouli-Bostanabad, Mohammad Barzegar-Jalali.
Project administration: Mohammad Barzegar-Jalali.
Resources: Mohammad Barzegar-Jalali.
Supervision: Mohammad Barzegar-Jalali.
Validation: Seraj Mohaghegh, Karim Osouli-Bostanabad.
Visualization: Mohammad Barzegar-Jalali.
Writing–original draft: Seraj Mohaghegh.
Writing–review & editing: Seraj Mohaghegh, Karim Osouli-Bostanabad, Hossein Nazemiyeh, Yadollah Omidi, Hossein Maleki-Ghaleh.

Competing Interests
The authors declare that they have no conflict of interest.

Research Highlights

What is the current knowledge?
- The AgNPs were synthesized through a green nanotechnology procedure using the extract of L. ruthenicum and citrate as a reducing agent.

What is new here?
- The optimization of pH value, concentration, and temperature of the reducing agent to synthesize AgNPs was studied.

Ethical Statement
There is none to be clarified.

Funding
There is none to be clarified.

References
1. Montalvo-Quiros S, Aragoneses-Cazorla G, Garcia-Alcalde L, Vallet-Regí M, González B, Luque-Garcia JL. Cancer cell targeting and therapeutic delivery of silver nanoparticles by mesoporous silica nanocarriers: insights into the action mechanisms using quantitative proteomics. *Nanoscale* **2019**; 11: 4531-45. doi: 10.1039/c8nr07667g.
2. Barbasz A, Oćwieja M, Roman M. Toxicity of silver nanoparticles towards tumoral human cell lines U-937 and HL-60. *Colloids Surf B Biointerfaces* **2017**; 156: 397-404. doi: 10.1016/j.colsurfb.2017.05.027.
3. Alfuraydi AA, Devanesan S, Al-Ansari M, AlSalhi MS, Ranjitsingh AJ. Eco-friendly green synthesis of silver nanoparticles from the sesame oil cake and its potential anticancer and antimicrobial activities. *J Photochem Photobiol B* **2019**; 192: 83-9. doi: 10.1016/j.jphotobiol.2019.01.011.
4. Nguyen-Tri P, Ouellet-Plamondon C, Rtimi S, Assadi AA, Nguyen TA. Methods for synthesis of hybrid nanoparticles. In: Mohapatra S, Nguyen TA, Nguyen-Tri P, eds. *Noble Metal-Metal Oxide Hybrid Nanoparticles*. Woodhead Publishing; **2019**. p. 51-63. doi: 10.1016/b978-0-12-814134-2.00003-6.
5. Borran AA, Aghanejad A, Farajollahi A, Barar J, Omidi Y. Gold nanoparticles for radiosensitizing and imaging of cancer cells. *Radiat Phys Chem* **2018**; 152: 137-44. doi: 10.1016/j.radphyschem.2018.08.010.
6. Lee SH, Jun BH. Silver nanoparticles: synthesis and application for nanomedicine. *Int J Mol Sci* **2019**; 20: 865. doi: 10.3390/ijms20040865.
7. Sánchez-López E, Gomes D, Esteruelas G, Bonilla L, Lopez-Machado AL, Galindo R, et al. Metal-based nanoparticles as antimicrobial agents: an overview. *Nanomaterials (Basel)* **2020**; 10: 292. doi: 10.3390/nano10020292.
8. Osouli-Bostanabad K, Aghajani H, Hosseinzade E, Maleki-Ghaleh H, Shakeri M. High microwave absorption of nano-Fe3O4 deposited electrophoretically on carbon fiber. *Mater Manuf Process* **2016**; 31: 1351-6. doi: 10.1080/10426914.2015.1090595.
9. Osouli-Bostanabad K, Hosseinzade E, Kianvash A, Entezami A. Modified nano-magnetite coated carbon fibers magnetic and microwave properties. *Appl Surf Sci* **2015**; 356: 1086-95. doi: 10.1016/j.apsusc.2015.08.115.
10. Mulfinger L, Solomon SD, Bahadory M, Jeyarajasingam AV, Rutkowsky SA, Boritz C. Synthesis and study of silver nanoparticles. *J Chem Educ* **2007**; 84: 322. doi: 10.1021/ed084p322.
11. Henglein A, Giersig M. Formation of colloidal silver nanoparticles: capping action of citrate. *J Phys Chem B* **1999**; 103: 9533-9. doi: 10.1021/jp9925334.
12. Kumar I, Mondal M, Sakthivel N. Green synthesis of phytogenic nanoparticles. In: Shukla AK, Iravani S, eds. *Green Synthesis,*

Characterization and Applications of Nanoparticles. Elsevier; **2019**. p. 37-73. doi: 10.1016/b978-0-08-102579-6.00003-4.
13. Gunalan S, Sivaraj R, Rajendran V. Green synthesized ZnO nanoparticles against bacterial and fungal pathogens. *Prog Nat Sci Mater Int* **2012**; 22: 693-700. doi: 10.1016/j.pnsc.2012.11.015.
14. Jamzad M, Kamari Bidkorpeh M. Green synthesis of iron oxide nanoparticles by the aqueous extract of *Laurus nobilis* L. leaves and evaluation of the antimicrobial activity. *J Nanostruct Chem* **2020**; 10: 193-201. doi: 10.1007/s40097-020-00341-1.
15. Rafique M, Sadaf I, Rafique MS, Tahir MB. A review on green synthesis of silver nanoparticles and their applications. *Artif Cells Nanomed Biotechnol* **2017**; 45: 1272-91. doi: 10.1080/21691401.2016.1241792.
16. Onitsuka S, Hamada T, Okamura H. Preparation of antimicrobial gold and silver nanoparticles from tea leaf extracts. *Colloids Surf B Biointerfaces* **2019**; 173: 242-8. doi: 10.1016/j.colsurfb.2018.09.055.
17. Anandan M, Poorani G, Boomi P, Varunkumar K, Anand K, Chuturgoon AA, et al. Green synthesis of anisotropic silver nanoparticles from the aqueous leaf extract of *Dodonaea viscosa* with their antibacterial and anticancer activities. *Process Biochem* **2019**; 80: 80-8. doi: 10.1016/j.procbio.2019.02.014.
18. Deepak P, Amutha V, Kamaraj C, Balasubramani G, Aiswarya D, Perumal P. Chemical and green synthesis of nanoparticles and their efficacy on cancer cells. In: Shukla AK, Iravani S, eds. *Green Synthesis, Characterization and Applications of Nanoparticles*. Elsevier; **2019**. p. 369-87. doi: 10.1016/b978-0-08-102579-6.00016-2.
19. Mohaghegh S, Osouli-Bostanabad K, Nazemiyeh H, Javadzadeh Y, Parvizpur A, Barzegar-Jalali M, et al. A comparative study of eco-friendly silver nanoparticles synthesis using *Prunus domestica* plum extract and sodium citrate as reducing agents. *Adv Powder Technol* **2020**; 31: 1169-80. doi: 10.1016/j.apt.2019.12.039.
20. Prabhu S, Poulose EK. Silver nanoparticles: mechanism of antimicrobial action, synthesis, medical applications, and toxicity effects. *Int Nano Lett* **2012**; 2: 32. doi: 10.1186/2228-5326-2-32.
21. Kumar V, Yadav SK. Plant-mediated synthesis of silver and gold nanoparticles and their applications. *J Chem Technol Biotechnol* **2009**; 84: 151-7. doi: 10.1002/jctb.2023.
22. Mukunthan KS, Balaji S. Cashew apple juice (*Anacardium occidentale* L.) speeds up the synthesis of silver nanoparticles. *Int J Green Nanotechnol* **2012**; 4: 71-9. doi: 10.1080/19430892.2012.676900.
23. El-Sherbiny IM, Salih E, Reicha FM. Green synthesis of densely dispersed and stable silver nanoparticles using myrrh extract and evaluation of their antibacterial activity. *J Nanostructure Chem* **2013**; 3: 8. doi: 10.1186/2193-8865-3-8.
24. Seeram NP. Berry fruits: compositional elements, biochemical activities, and the impact of their intake on human health, performance, and disease. *J Agric Food Chem* **2008**; 56: 627-9. doi: 10.1021/jf071988k.
25. Miller JS. Phylogenetic relationships and the evolution of gender dimorphism in *Lycium* (Solanaceae). *Syst Bot* **2002**; 27: 416-28. doi: 10.1043/0363-6445-27.2.416.
26. Levin RA, Miller JS. Relationships within tribe Lycieae (Solanaceae): paraphyly of *Lycium* and multiple origins of gender dimorphism. *Am J Bot* **2005**; 92: 2044-53. doi: 10.3732/ajb.92.12.2044.
27. Hu N, Zheng J, Li W, Suo Y. Isolation, stability, and antioxidant activity of anthocyanins from *Lycium ruthenicum* Murray and *Nitraria tangutorum* Bobr of Qinghai-Tibetan Plateau. *Sep Sci Technol* **2014**; 49: 2897-906. doi: 10.1080/01496395.2014.943770.
28. Gong Y, Wu J, Li ST. Immuno-enhancement effects of *Lycium ruthenicum* Murr. polysaccharide on cyclophosphamide-induced immunosuppression in mice. *Int J Clin Exp Med* **2015**; 8: 20631-7.
29. Ni W, Gao T, Wang H, Du Y, Li J, Li C, et al. Anti-fatigue activity of polysaccharides from the fruits of four Tibetan Plateau indigenous medicinal plants. *J Ethnopharmacol* **2013**; 150: 529-35. doi: 10.1016/j.jep.2013.08.055.
30. Wang H, Li J, Tao W, Zhang X, Gao X, Yong J, et al. *Lycium ruthenicum* studies: molecular biology, phytochemistry and pharmacology. *Food Chem* **2018**; 240: 759-66. doi: 10.1016/j.foodchem.2017.08.026.
31. Chahardoli A, Karimi N, Fattahi A. *Nigella arvensis* leaf extract mediated green synthesis of silver nanoparticles: their characteristic properties and biological efficacy. *Adv Powder Technol* **2018**; 29: 202-10. doi: 10.1016/j.apt.2017.11.003.
32. Das P, Ghosal K, Jana NK, Mukherjee A, Basak P. Green synthesis and characterization of silver nanoparticles using belladonna mother tincture and its efficacy as a potential antibacterial and anti-inflammatory agent. *Mater Chem Phys* **2019**; 228: 310-7. doi: 10.1016/j.matchemphys.2019.02.064.
33. Terenteva EA, Apyari VV, Dmitrienko SG, Zolotov YA. Formation of plasmonic silver nanoparticles by flavonoid reduction: a comparative study and application for determination of these substances. *Spectrochim Acta A Mol Biomol Spectrosc* **2015**; 151: 89-95. doi: 10.1016/j.saa.2015.06.049.
34. Rajeshkumar S, Malarkodi C, Gnanajobitha G, Paulkumar K, Vanaja M, Kannan C, et al. Seaweed-mediated synthesis of gold nanoparticles using *Turbinaria conoides* and its characterization. *J Nanostructure Chem* **2013**; 3: 44. doi: 10.1186/2193-8865-3-44.
35. Yang N, Wei XF, Li WH. Sunlight irradiation induced green synthesis of silver nanoparticles using peach gum polysaccharide and colorimetric sensing of H2O2. *Mater Lett* **2015**; 154: 21-4. doi: 10.1016/j.matlet.2015.03.034.
36. Ahmad T, Bustam MA, Irfan M, Moniruzzaman M, Asghar HM, Bhattacharjee S. Mechanistic investigation of phytochemicals involved in green synthesis of gold nanoparticles using aqueous *Elaeis guineensis* leaves extract: role of phenolic compounds and flavonoids. *Biotechnol Appl Biochem* **2019**; 66: 698-708. doi: 10.1002/bab.1787.
37. Dauthal P, Mukhopadhyay M. Noble metal nanoparticles: plant-mediated synthesis, mechanistic aspects of synthesis, and applications. *Ind Eng Chem Res* **2016**; 55: 9557-77. doi: 10.1021/acs.iecr.6b00861.
38. Kytsya A, Bazylyak L, Hrynda Y, Horechyy A, Medvedevdkikh Y. The kinetic rate law for the autocatalytic growth of citrate-stabilized silver nanoparticles. *Int J Chem Kinet* **2015**; 47: 351-60. doi: 10.1002/kin.20913.
39. Yang Z, Qian H, Chen H, Anker JN. One-pot hydrothermal synthesis of silver nanowires via citrate reduction. *J Colloid Interface Sci* **2010**; 352: 285-91. doi: 10.1016/j.jcis.2010.08.072.
40. Philip D. Green synthesis of gold and silver nanoparticles using *Hibiscus rosa-sinensis*. *Physica E Low Dimens Syst Nanostruct* **2010**; 42: 1417-24. doi: 10.1016/j.physe.2009.11.081.
41. Sharma VK, Yngard RA, Lin Y. Silver nanoparticles: green synthesis and their antimicrobial activities. *Adv Colloid Interface Sci* **2009**; 145: 83-96. doi: 10.1016/j.cis.2008.09.002.